Technological aspects in blanket design: Effects of micro-alloying and thermo-mechanical treatments of EUROFER97 type steels after neutron irradiation

M. Rieth[1], E. Simondon[1*], G. Pintsuk[2], G. Aiello[3], J. Henry[4], D. Terentyev[5], A. Puype[6], C. Cristalli[7], L. Pilloni[8], O. Tassa[9], M. Klimenkov[1], H.-C. Schneider[1], P. Fernandez[10], T. Gräning[11], X. Chen[11], A. Bhattacharya[11], J. Reed[11], J.W. Geringer[11], M. Sokolov[11], Y. Katoh[11], L. Snead[12]

[1]Karlsruhe Institute of Technology, IAM-AWP, Hermann-von-Helmholtz-Platz 1, 76344 Eggenstein-Leopoldshafen, Germany
[2]Forschungszentrum Jülich GmbH, Institut für Energie- und Klimaforschung – Plasmaphysik, 52425 Jülich, Germany
[3]EUROfusion, PPPT, 85748 Garching, Germany
[4]Université Paris-Saclay, CEA, Service de Recherches Métallurgiques Appliquées, 91191, Gif-sur-Yvette, France
[5]Belgian Nuclear Research Centre, SCK•CEN, Mol, 2400, Belgium
[6]OCAS NV, Pres. J.F. Kennedylaan 3, 9060 Zelzate, Belgium
[7]ENEA, Brasimone, Camugnano, BO 40032, Italy
[8]ENEA CR CASACCIA, Via Anguillarese 301, 00123 Rome, Italy
[9]Centro Sviluppo Materiali S.p.A., Via di Castel Romano 100, 00128 Roma, Italy
[10]National Fusion Laboratory, CIEMAT. Avenida Complutense, 40., Madrid, Spain
[11]Oak Ridge National Laboratory, Oak Ridge, TN 37831-6115, USA
[12]Irradiation Materials Sciences Consulting (IMSC), 206 S. Country Road, Bellport NY 11713, USA

*Corresponding author: esther.simondon@kit.edu

Referee suggestions:

- Shuhei Nogami, shuhei.nogami.d3@tohoku.ac.jp
- Christian Linsmeier, ch.linsmeier@fz-juelich.de
- Mike Gorley, mike.gorley@ukaea.uk
- Sergei Dudarev, sergei.dudarev@ukaea.uk
- Eberhard Diegele, eberhard.diegele@euro-fusion.org
- Anton Möslang, anton.moeslang@kit.edu

Abstract

Presently available data on neutron irradiation damage raise doubts on the feasibility of using EUROFER97 steel for a water-cooled starter blanket in a DEMO reactor, since the ductile-to-brittle transition temperature (DBTT) increases significantly for irradiation temperatures below 350°C. The additional DBTT shift caused by H and He transmutation can only be estimated based on very few results with isotopically tailored EUROFER97 steel. Conservative calculations show that the DBTT of EUROFER97 steel could exceed the operating temperature in water-cooled starter blankets within a relatively short time period. This paper presents results from a EUROfusion funded irradiation campaign that was performed in the High Flux Isotope Reactor at Oak Ridge National Laboratory. The paper compares ten newly developed reduced activation ferritic-martensitic (RAFM) steels irradiated to a dose of 2.5 dpa at 300°C. The post-irradiation experiments using Small Specimen Test Technology included hardness, tensile, and fracture mechanics tests combined with fractography and microstructure analysis are presented. Results show that micro-alloying EUROFER97-type steels influenced the mechanical properties but a dominating impact on irradiation damage resistance could not be identified. In contrast, specific thermo-mechanical treatments lead to better DBTT behavior. Discussion about irradiation response to heat treatment conditions is also given. Despite requiring data also at high dpa values, the results indicate that with these modified materials an increased lifetime and potentially also an increased operating temperature window can be achieved compared to EUROFER97.

Keywords

EUROFER97
thermo-mechanical treatment
neutron irradiation
post irradiation examination
embrittlement
fracture toughness

1. Introduction

The most problematic material-related challenge for DEMO and future commercial fusion power plants concerns the mitigation of neutron damage, that is, embrittlement by irradiation-induced defects and transmutation of helium and hydrogen. It has the highest impact on the design and licensing of blanket and divertor structures. As of today, the assumed design limits are highly speculative, even for a starting configuration with rather moderate performance.

Different operational environments are foreseen for the blanket and divertor of the first DEMO reactor related to their temperature handling requirements as well as the expected neutron damage level. While for the divertor, water cooling at ~180°C is foreseen, two different design options for the breeding blanket are considered. On the one hand, this is the “water-cooling” option which implies a minimum irradiation temperature for the blanket material in the range of 280-350°C. On the other hand, the “helium-cooled” and “dual-coolant” solutions imply a maximum operating temperature for the blanket material in the range of 650°C.

Concerning the water-cooling options for the divertor and the blanket, presently available data on irradiation damage limit the allowed dose to ~6 dpa and raise doubts on the feasibility of using EUROFER97 steel for a water-cooled starter blanket in a DEMO reactor. Indeed, the ductile-brittle transition temperature (DBTT) of this material increases significantly for irradiation temperatures below 350°C. This DBTT shift is caused on the one hand by created microstructural defects and on the other hand by transmutation (H and He production). While the effect of microstructural defects

can be simulated by fission neutron irradiation, transmutation effects can only be estimated using isotopically tailored EUROFER97 steel for which yet only few results from one irradiation campaign are available [1], [2]. Conservative calculations suggest that the DBTT of EUROFER97 steel would exceed the operating temperature in water-cooled starter blankets within a relatively short time.

Concerning the helium-cooling option, the moderate heat transfer of He will maintain the temperatures in the EUROFER97 structures at and above 350°C, which would guarantee moderate irradiation-induced DBTT shifts mainly related to material transmutation, especially in high dpa regions of the blanket like the first wall. Recent R&D points to the possibility to extend the high temperature operating limit of EUROFER97 to over 550°C [3]–[5]. Albeit preliminary, these results, if confirmed, would allow an increase in the outlet temperature of the coolant improving the reactor net efficiency [6]. Unfortunately, the improvement on the high-temperature end is often accompanied by an increase of the DBTT at the lower end in the non-irradiated state, and with He-transmutation induced embrittlement, the DBTT could reach room temperature comparably fast.

In summary, DEMO design assessment requires further experimental data on H and He transmutation effects and risk-mitigation action on advanced material development is required. Regarding the latter, after more than four years, the EUROfusion funded irradiation screening campaign on advanced RAFM steel grades, performed in the High Flux Isotope Reactor (HFIR) at Oak Ridge National Laboratory (ORNL), was recently completed. **The work focuses on the development of innovative RAFM steels able to withstand the critical temperatures typical of the different operational environments foreseen for the blanket of the first DEMO reactor**. Therefore, in this study, the following questions were addressed:

- How do specific thermo-mechanical treatments and modest changes of chemical specifications (i.e., micro alloying) influence the irradiation behavior? Which strategies are promising? Which materials or approaches can be down-selected?
- How meaningful is small specimen test technology compared to results from international test standards?
- How does a technologically relevant heat treatment change the irradiation properties of EUROFER97?

This campaign included ten materials of EUROFER97/2 and EUROFER-type that have been irradiated to a dose of 2.5 dpa at 300°C, in geometries yielding mechanical properties that are relevant and necessary for a comparison and possible down-selection of some grades from the advanced steels development program. For a meaningful assessment of the materials, the post-irradiation experiments were restricted to basic properties like hardness, tensile, and fracture mechanics tests combined with fractography and TEM analysis.

2. Experimental

2.1. Materials and strategy

Ten materials were selected to be irradiated in this study. They were derived from the optimization processes, targeting to expand the in-service temperature window of EUROFER97/2. These optimization processes consist of changing the processing route or the chemical composition with respect to EUROFER97/2 to improve selected, specific properties like creep strength, toughness, and low-temperature embrittlement in the unirradiated state. The present study was performed to determine the effect of neutron irradiation on these RAFM steels. The chemical compositions (real compositions measured by chemical analysis) of the ten steels are given in Table 1, and the details of the thermo-mechanical treatments (TMT) and heat treatments of their production process are given

in Table 2. The materials were produced as 100 kg lab-casts in the vacuum induction furnace at OCAS NV.

Material E refers to the second industrially produced EUROFER97/2 heat 993391. However, after production in the as-received state, an austenitization at 980°C was performed, followed by a very slow cooling down to room temperature (RT) over 24 h. Then, a standard heat treatment with an austenitization at 980°C, an air quench and a tempering at 760°C were performed. This treatment is called 'technological treatment', as it simulates the worst-case technological situation, which could occur after welding or during problematic production steps. This off-normal case is not a standard EUROFER, but rather covers the lower range of EUROFER material properties.

Materials H, I and P varied in terms of composition compared to EUROFER97/2 as well as of the production route. The ingots were reheated to a temperature of 1150°C for 1 h after which they were rolled in 4 rolling passes at pre-defined decreasing temperatures of 1100°C, 1050°C, 1000°C, 950°C and a then in 4 passes in a final rolling temperature of 900°C with a reduction of 16% per pass, to a final thickness of 20 mm. This TMT was followed by extreme (non-standard) austenizing and tempering treatments. The reduction of C is meant to reduce the amount of $M_{23}C_6$ precipitation, the addition of V and N is supposed to promote VN precipitation and the withdrawal of Mn is bound to increase the austenite formation temperature and therefore increase the possible upper tempering temperature range. These three materials (H, I, P) have been studied in earlier works (then called J362, J363 and J361, respectively) [3].

For material J, also tagged as 'lab-cast EUROFER' in earlier works [5], the production process comprised a TMT alternative to EUROFER97/2: the ingot was reheated to a temperature of 1250°C for 1 h after which it was rolled in 6 rolling passes at pre-defined decreasing temperatures of 1200°C, 1150°C, 1100°C, 960 C, 900°C and a final rolling temperature of 850°C with a reduction of 20–30% per pass, to a final thickness of ~11 mm. This TMT was followed by a tweaked quenching and tempering treatment. This resulted in a good mechanical performance, with a DBTT of -147°C, based on the KLST Charpy impact test results [5], while maintaining similar tensile properties as EUROFER97/2 in the high temperature application region. Therefore, this material delivers optimum properties and can be considered as the optimum state of EUROFER in terms of fabrication, thermomechanical treatment and heat treatment.

Concerning K-grade, its composition was altered w.r.t. EUROFER97/2 to improve low temperature performance by eliminating elements such as Mn that contribute to dislocation loop formation during irradiation due to irradiation induced segregation and trapping effects. K-material has undergone similar TMT and rolling passes as the J-grade, but the post-rolling thermal treatment was adjusted to avoid ferrite formation during Q&T as both carbon, chromium and manganese content were reduced.

Material L received a special heat treatment. The strategy for selecting the conditions was (i) to increase the austenizing temperature (up to 1150°C) in order to maximize the dissolution of precipitates, and (ii) to lower the tempering temperature, so as to increase the number density of carbo-nitrides which precipitate during tempering. The austenizing temperature was selected based on THERMOCALC calculations, with the aim to avoid complete dissolution of Ta-rich carbo-nitrides and therefore excessive austenite grain growth. While the applied special heat treatment was not designed to improve the behavior after irradiation at temperatures below 350°C, material L was nevertheless included in the HFIR irradiation campaign in order to assess the effect of special heat treatments on the mechanical performances after low temperature irradiation, in comparison with standard EUROFER and heats designed for low temperature applications.

Material M refers to the industrially produced second EUROFER97/2 batch (heat number 993391). After a standard hot rolling, it was submitted to a double normalizing at 1020°C and then tempering at 760°C. This double austenitization treatment has been chosen, after a study on multiple austenitizations at different temperatures, to optimize the prior austenite grain (PAG) size reduction. This successfully reduced the PAG size by approximately 25% compared to a standard heat treatment of EUROFER97/2, and consequently increased the toughness by decreasing the DBTT by about 7°C (KLST samples) [7].

Material N contains a reduced N content (0.002 %) and has suppressed V content, in order to reduce secondary precipitation. This makes it a 9Cr1WTa type alloy. As for M, a double austenitization stage has then also been applied, but at lower temperature (920°C), because it was noticed that the PAG size stayed stable even for markedly lower normalization temperatures. The heat treatment was then completed by a standard tempering (760°C). This alloy performed slightly better in DBTT compared to EUROFER97/2 with standard thermal treatment, but the tensile properties proved lower [8].

Material O is an alloy with increased content of N (up to 0.07 %) and V (up to 0.3 %) and decreased content of C (0,06 %) and Ta (0,05%) in order to reduce the precipitation of $M_{23}C_6$ and to foster the precipitation of V and Cr nitrides, whose dimensions are expected to be lower than the previous ones [9]. The material was submitted to a processing specific to the high temperature applications alloys, consisting of three stages: (i) a normalization at 1080°C. This higher temperature was chosen in order to keep the PAG size in a range of 50-70 microns, thought to be sufficient to grant creep resistance and, at the same time, not to be so detrimental for toughness. (ii) An ausforming with 40% section reduction ratio rolling at 650°C, in order to gain a carbo-nitride precipitation meant to "pin" the dislocations net (iii) and a final standard tempering at 760°C. Initially developed for high temperature operation, material O has been discarded due to poor creep resistance (among the tested alloys) [8]. However, it is still considered as an option for low temperature applications because of its good impact properties.

M-code	Cr	C	Mn	V	N	W	Ta	Si	Provider
E	**8.83**	**0.107**	**0.53**	**0.20**	**0.019**	**1.08**	**0.12**	**0.04**	**KIT**
H	8.70	0.058	0.02	0.35	0.047	1.07	0.10	0.04	
I	8.73	0.110	0.02	0.35	0.042	1.08	0.09	0.04	
P	8.70	0.105	0.02	0.2	0.045	1.14	0.09	0.03	
J	9.00	0.107	0.39	0.22	0.022	1.10	0.11	<0.04	**SCK.CEN**
K	7.84	0.017	<0.03	0.22	0.022	0.99	0.13	<0.04	
L	9.14	0.106	0.54	0.20	0.038	1.11	0.12	0.03	**CEA**
M	**8.83**	**0.107**	**0.53**	**0.20**	**0.019**	**1.08**	**0.12**	**0.04**	**ENEA**
N	9.04	0.092	0.11	<0.05	0.002	0.99	0.09	0.04	
O	8.8	0.06	0.50	0.3	0.07	0.97	0.05	0.15	

Table 1: Chemical compositions of 10 different Eurofer-97 steel variants. All values are in wt.%. E and M = reference EUROFER97/2 (Heat 993391). L = EUROFER97/2 (Heat 994578)

M-Code	Condition	Provider
E	'Technological treatment' : 980°C/ + slow AC + 980°C/0.5h + AQ + 760°C + AC	KIT
H	TMT: 1150°C and then rolling in 8 steps down to a final rolling temperature of 900°C with a reduction of 16% for each rolling step, then WQ.	
I		
P	1000°C/0.5h + WQ + 820°C/2h + AC in air	
J	TMT:1250°C/1h and then rolling to a final rolling temperature of 850°C in 6 rolling steps with a reduction of 20-30% for each rolling pass, then AC.	SCK.CEN
	880°C/0.5h + WQ + 750°C/2h + AC in air	
K	TMT:1250°C/1h and then rolling to a final rolling temperature of 850°C in 6 rolling steps with a reduction of 20-30% for each rolling pass, then AC.	
	1050°C/15min + WQ + 675°C/1.5h + AC	
L	1150°C/0.5h + WQ + 700°C/1.5h+ AC	CEA
M	1020°C/0.5h + AQ + 1020°C/0.5h + AQ +760°C/1.5h + AC (double austenitization)	ENEA

N	920°C/1.5h + AQ + 920°C/1.5h + AQ + 760°C/1h + AC (double austenitization)	
O	TMT: 1080°C/1h, cooling to 650°C and rolling, reduction 40% (from 30 mm to 18mm) Tempering: 760°C/1h + AC	

Table 2: Summary of different processing conditions submitted to Eurofer-97 steel variants. AQ: air quenched, WQ: water quenched, AC: Air Cooling, HT: high temperature, LT: low temperature

2.2. Irradiation

The irradiation program has been undertaken in the High-Flux-Isotope-Reactor (HFIR) at the Oak Ridge National Laboratory (ORNL). The fast neutron (E > 0.1 MeV) fluence is 3.1×10^{25} m^{-2} and the fluxes are in the range 0.66 to 1.1×10^{19} $n/m^2/s$, which approximately corresponds to 4.7 to 7.9×10^{-7} dpa/s for 9% Cr RAFM steels (like EUROFER). HFIR is a mixed spectrum reactor in which the thermal-to-fast neutron flux ratio is approximately 2.1 throughout the core including the Flux Trap. Materials have been irradiated for 3 months to the average dose of 2.5 ± 0.25 dpa at the target temperature of 300°C ± 30°C, in the shape of sub-sized tensile specimens (SS-J3) and 4-notch fracture toughness bend bar specimens (M4CVN) placed in rabbit capsules. The temperature of irradiation was determined based on Finite Element Analysis (FEA). It was calibrated by the thermometry readings from silicon carbide (SiC) temperature monitors irradiated in direct contact with the specimens. The temperature monitor reading was carried out primarily by the dilatometry method. Irradiation temperature measurements using SiC thermometry specimens has been described in detail by Campbell et al. [10]. The temperature of irradiation is expected to be stable within ±4% of of the difference between the design temperature (T_{des}) and the coolant temperature (T_c, ~60°C) during the full power operation, i.e., ±10°C for rabbits designed for 300°C. It typically takes about a day for HFIR to ramp up to the full power upon start-up. The shutdown process is much quicker. The holder assembly temperature reaches the equilibrium within a few minutes after the reactor reaches each power step.

For tensile specimens, a total of 40 specimens (4 per material) were irradiated in two different capsules. In the end, only samples with an evaluated irradiation temperature within the desired range (300 ± 30°C) were selected for post irradiation evaluation (hardness and tensile tests). Additionally, Vickers hardness measurements were used as a cross-check on the tensile samples temperatures by highlighting any material showing abnormal behavior and therefore acted as an added guide to select appropriate samples for further analysis. For each material, the Vickers hardness did not show dependency on the irradiation temperature.

For bend bars, a total of 20 specimens (2 per material) were irradiated in five different capsules. The irradiation temperature for each SiC cut specimen was determined based on the deformation measurements in a dilatometer [10]. For each test, the mean value of the minimum and maximum temperatures was used as the irradiation temperature for the cut thermometry specimen. The average irradiation temperatures calculated are reported in Figure 1. Considering ± 20°C uncertainties in the irradiation temperature determination by SiC specimens (error bars), most bend bar specimens achieved the target irradiation temperature range of 300 ± 30°C. However, materials M and N in the capsule ES34 experienced much higher irradiation temperature of ~476 °C. Therefore, these materials were excluded from the study, i.e. the results of further examinations of these bend bars are not presented. As for materials K and L, their lower irradiation temperature must be considered and cared for in the interpretation of results, even though it is not supposed to have a big influence, since irradiation hardening/embrittlement generally is expected to saturate when T <~ 350 °C [2]. In other words, as long as the irradiation temperature is lower than ~350 °C, the hardening behavior for a fixed dose will not be drastically different.

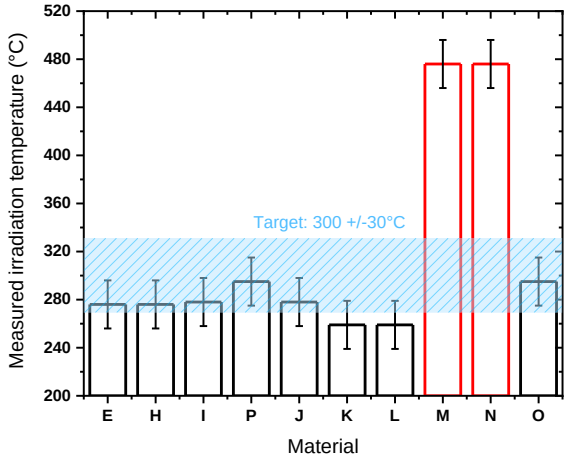

Figure 1 : Irradiation temperature measurements for bend bar specimens. The blue range represents the target temperature of irradiation. The scatter band corresponds to the error on the SiC thermometry measurement of +/-20°C.

2.3. Characterizations

Microscopy. Microstructure of the as-received samples was characterized at multi length scales using light optical microscopy (LOM), scanning electron microscopy (SEM) and transmission/scanning-transmission electron microscopy (TEM/STEM). LOM was performed on the undeformed head/grip sections of the broken tensile samples after the tensile tests polished with mirror quality. SEM was performed on the same samples after etching in Villela's reagent. A field emission gun (FEG) based Hitachi S4800 SEM was used.

TEM. TEM specimens were lifted out by focused ion beam (FIB) from tab region of broken tensile test articles. TEM/STEM characterization of the irradiated samples was performed using a XFEG based FEI F200X Talos STEM operating at 200 kV, equipped with high resolution STEM detectors and a FEI 4096×4096 resolution "Ceta" CCD camera. The imaging of precipitate phases was performed by high-count rate EDX mapping of the samples using FEI F200X Talos STEM. Thickness measurements of the foils, needed to estimate defect densities, was performed using a FEG based JEOL 2100F TEM equipped with a Gatan GIF EELS spectrometer. Readers are referred to [11] for more details on microstructure characterization technique.

Hardness. Vickers microhardness indentation tests were performed on irradiated tensile and toughness specimens in accordance with ASTM E384 Standard Test Method for Microindentation Hardness of Materials, using 1 kg load, 15 s dwell time, at room temperature. These tests were conducted using a Mitutoyo HV-120 hardness tester. For the M4CVN samples, the indentations were performed adjacent to the end of fatigue precrack, at least 4 indents per notch, while the indentations were made on the head/grip section of SS-J3 tensile specimens. For SS-J3 specimens, a minimum of 6 indents per sample were measured to provide an average hardness value of each steel. All the irradiated samples were tested because Vickers hardness measurements can serve as a cross-check on the sample temperatures by highlighting any material showing abnormal hardness behavior.

Tensile tests. Tensile tests were carried out on type SS-J3 miniature tensile specimens using a strain rate of 10^{-3} s^{-1} in shoulder loading configuration and using the machine stroke for estimating elongation, following the standard procedure guidelines provided in ASTM E8/E8M-15a. Tests were performed at room temperature (RT) and 300 °C using an Instron 3367 tensile machine equipped with a 5 kN load cell. Elevated temperature tests were conducted in high vacuum environment. Load and strain data were digitally recorded and analyzed. Fracture surfaces were examined using JEOL JSM-6010LA scanning electron microscope.

Toughness tests. Three-point bending testing was carried out on type M4CVN miniature bending bar specimens of dimension 45×3.3×1.65 mm with 4 notches, i.e. 4 tests can be performed per specimen. The specimens have been pre-cracked prior to irradiation. Tests on the irradiated samples were performed in an enclosed chamber with heating bands for elevated temperature testing or liquid nitrogen cooling for low temperature testing. Fracture toughness K_{Jc} as well as the reference fracture toughness T_{0Q} were determined in the transition region according to ASTM Standard E1921 Master Curve Method. More details on toughness testing are available in [12].

3. Results

3.1. Microstructure

SEM and TEM investigations were performed on all materials before irradiation. Materials H, I, P and K were also investigated after irradiation by TEM. Selected results here are presented to give an overview of the microstructural features, linked to chemical composition and performed heat treatments. Complete microstructure results can be found in [13]. Figure 2 presents the optical images of etched samples of the materials. Most materials show the typical appearance of a tempered ferritic-martensitic (F-M) steel with PAGs, laths and precipitates decorating laths.

Material E displays larger PAGs than the standard EUROFER97, and also presents a non-uniform distribution of very coarse precipitates (> 1µm), expected to be carbides. Their presence is evident on Figure 3, an SEM image of a relatively deep etched surface of sample E. Such coarse precipitates are uncharacteristic of EUROFER97/2 and unexpected in any 9%Cr F-M steel under conventional heat treatment condition (980-1050°C austenitization and 700-780°C tempering) [14]. Their presence is attributed to the off-normal heat treatment that E was subjected to.

For materials H and I, the microstructures seem to be slightly over-tempered. They contain a small fraction of ferrite grains, indicated in Figure 2 by arrows. They appear much brighter in the etched steels without much carbides (black dots). Also, it is evident from Figure 2 that H series steel has larger grains as compared to I and P.

J-series steel displays the finest microstructure, due to the optimized ausforming and low austenitization temperature of 880°C.

K series consists on the contrary of very large PAGs, with a bimodal grain size, which can be attributed to the high normalizing temperature (1050°C) and prior thermomechanical processing. Its overall microstructure appears to be under-tempered, with yet not fully developed lath structures. Figure 2 shows martensitic regions much brighter than tempered areas after etching, because the carbides have not yet formed in these regions. This is expected because the tempering temperature of material K is 675°C, which is very low compared to usually 750-760°C for F-M steels.

Material L has the typical microstructure expected for tempered F-M steel, but with very large PAGs (>50 µm), which is the result of the very high austenitization temperature (1150°C).

Material O is comprised of elongated grains along the plate rolling direction, which is expected due to the hot rolling at 650°C with 40% reduction.

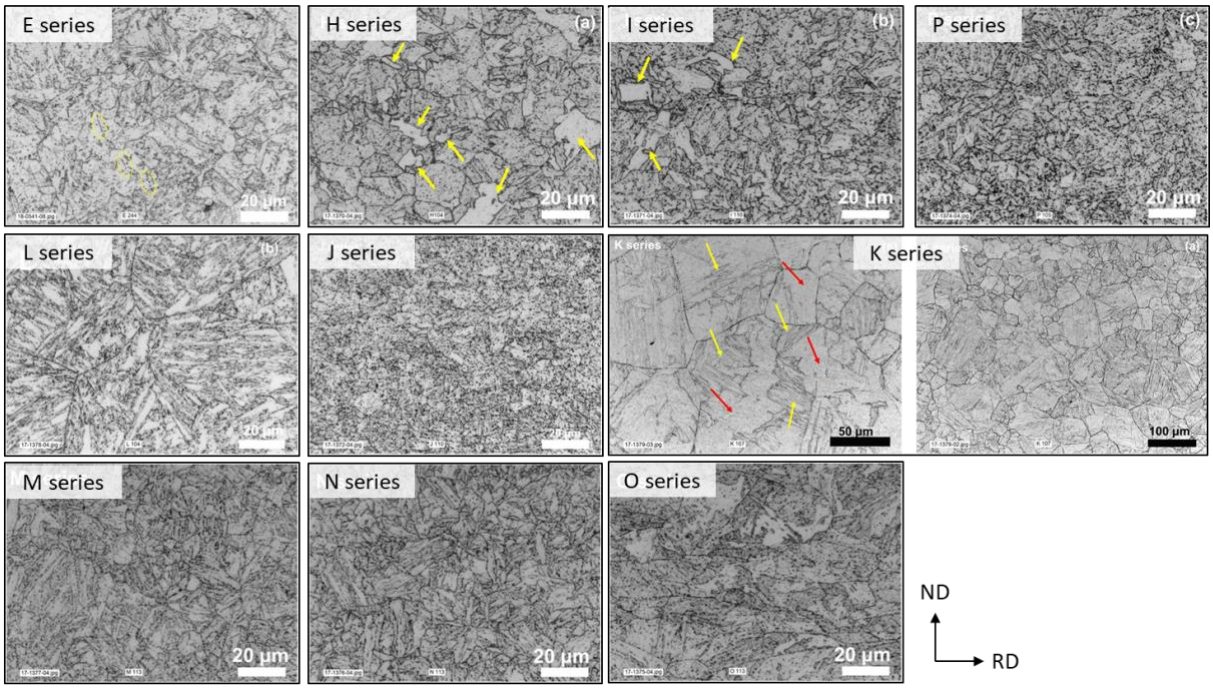

Figure 2: Light Optical Microscopy images of the unirradiated materials after etching in Villela's reagent. RD = rolling direction. ND = normal direction.

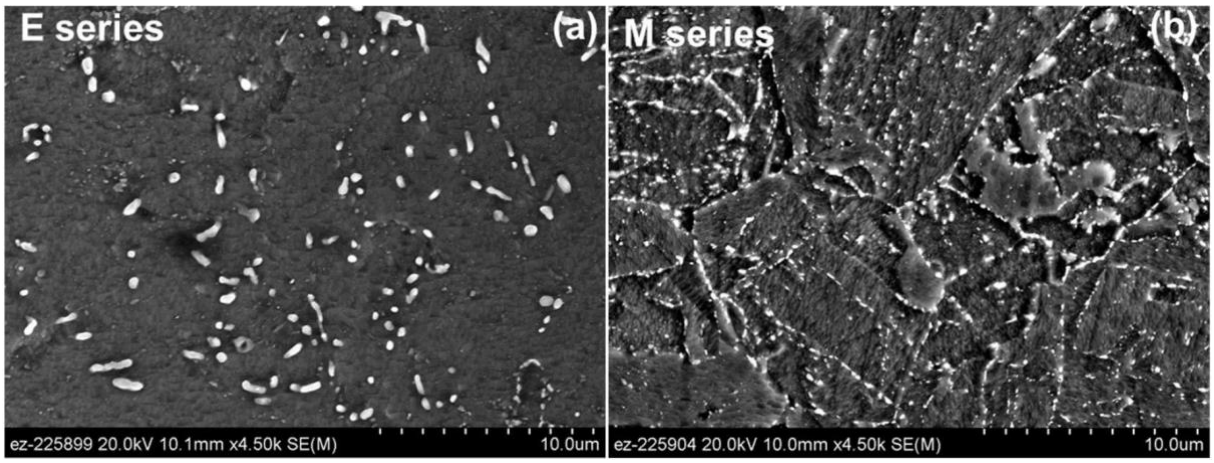

Figure 3: SEM images of unirradiated materials a) E and b) M at the same magnification after deep etching highlighting the presence of coarse carbides in E series

Regarding the precipitation, most materials present two types of precipitate families: (i) predominantly Ta, V and N rich precipitates, which are expected to be the MX carbo-nitride precipitates and (ii) predominantly Cr, W rich phases, which are expected to be $M_{23}C_6$ carbides. In material K, however, an evident lack of precipitates is observed as a result of the very low C content of this material. Material L presents a density of precipitates comparable to most others, including $M_{23}C_6$, but previous work showed that this steel mainly contained Cr and V rich M_2X nitrides instead of MX carbo-nitrides [15].

After neutron irradiation, conventional and analytical STEM was performed on focused ion beam (FIB) lift out foils obtained yet only from irradiated samples of the materials H, I, P and K. The samples were taken from slivers cut from the irradiated and tensile tested samples. The location of the samples was taken from the head/grip section where no severe plastic deformation due to the tensile testing was expected.

The STEM-EDX mapping investigations have not revealed any significant modification of the pre-existing features (PAG, block, lath sizes and precipitation state) after the irradiation. H, I and P materials presented no significant change in the precipitate structure, and material K still presented a lack of precipitates. Medium angle annular dark field (MAADF) and associated EDX maps have also

shown no evidence of any chemical re-distribution or secondary phase precipitation of any sort. Hence, the pre-existing microstructures appear stable against irradiation at the given irradiation conditions. This is to be expected considering the rather low dose of 2.5 dpa. However, some particular features induced by irradiation were noticed, such as complex sponge-like structures, pure Cr-rich precipitates and Cr enriched areas. Details of these observations can be found in [16].

After performing analytical analysis of the secondary phases, STEM-BF and low angle annular dark field (LAADF) imaging was used to study the irradiation induced extended defects. This revealed that dislocation loops had formed in the steels due to irradiation. Figure 4 shows the corresponding BF and LAADF images for materials H and K, imaged close to [101] zone axis. Some of the identified dislocation loops are encircled in the LAADF image. The dislocation loop microstructure is quite complex as both individual and tangling loops are observed. Many loops are located nearby dislocation lines pointing at the decoration effect originating from the elastic interaction and the fact that loops exhibit diffusion during irradiation. The diffusion of small loops may also explain the presence of rather large loops, apparently formed as a result of loop coalescence. Numerous individual loops were identified but many loops were seen interacting with dislocation lines and/or with neighboring loops. Although the g.b analysis was not performed, from the considerable amount of knowledge on irradiation induced microstructure in RAFM steels and 9Cr alloys, the loops with a 1/2<111> Burgers vector are expected. The average diameter and number density of the dislocation loops (black dots of uncertain origin were excluded from the analysis) is reported in Table 3. For materials H, I and P, the size of the loops is very small, between ~2-6 nm in diameter. Such small dislocation loops are remarkably different to the results obtained in the K series steel, where the average loop size (11 nm) and the number of loops were much larger. Here, one must be cautious that the loop sizes in H series steel are very close to those expected from FIB damage. Additional microstructural investigations with higher nanoscale resolution on newly prepared samples will be carried out to confirm the observations and extend it to all the materials of the study.

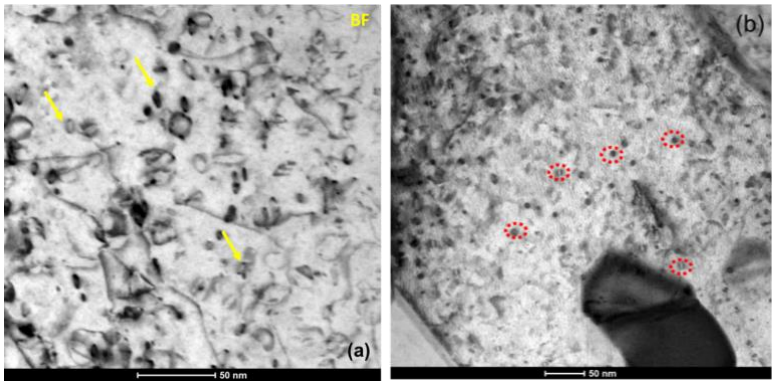

Figure 4: STEM-BF images revealing the dislocation loops in irradiated steels (a) K-series, (b) P-series. Imaging performed close to (a) [001] zone axis using a <110> type g vector and (b) [101] zone axis, in down axis condition

Material	Average diameter	Number density
H	~ 3 nm	1.2×10^{21} m^{-3}
I	~ 4 nm	2.3×10^{21} m^{-3}
P	~ 6.7 nm	5.5×10^{20} m^{-3}
K	~ 11 nm	1.8×10^{22} m^{-3}

Table 3: Mean size of the dislocation loops and their number density (assuming ~150 nm sample thickness)

3.2. Vickers microhardness

Vickers hardness indentation tests were performed before and after irradiation on all the steel variants on the head/grip section of SS-J3 tensile samples (Figure 5). The results before irradiation show that K- and L-series steels have the highest hardness, exceeding 300 HV, while all the other

steels did not deviate from 200-220 HV, in line with the values of unirradiated EUROFER97/2 (treated with 980 °C/air + 760 °C/air), i.e., around 220 HV [17]. This difference could be attributed to the much lower tempering temperatures for both K- and L steels. L-series steel was tempered at 700°C and the K-series steel was tempered at 675°C, which are both significantly lower than the tempering temperature of ~760°C used for reference EUROFER97/2 steels. Material H is the softest, with an average Vickers hardness of only 192 HV. Compared to materials with the same heat treatment, the drop of strength could be attributed to the withdrawal of elements such as C, having a role in precipitation hardening ($M_{23}C_6$), as well as in solution hardening,

After irradiation, all the alloys, independent on their processing routes and modified minor-alloying chemistries, showed hardening. The hardest steels are still the K- and L-series steels with values higher than 400 HV. The hardness of all the other steels stayed lower than 310 HV. In comparison of materials E and J, which exhibit the same hardness before irradiation, E shows less hardening and is in the end a bit softer, which is attributed to its off-normal heat treatment.

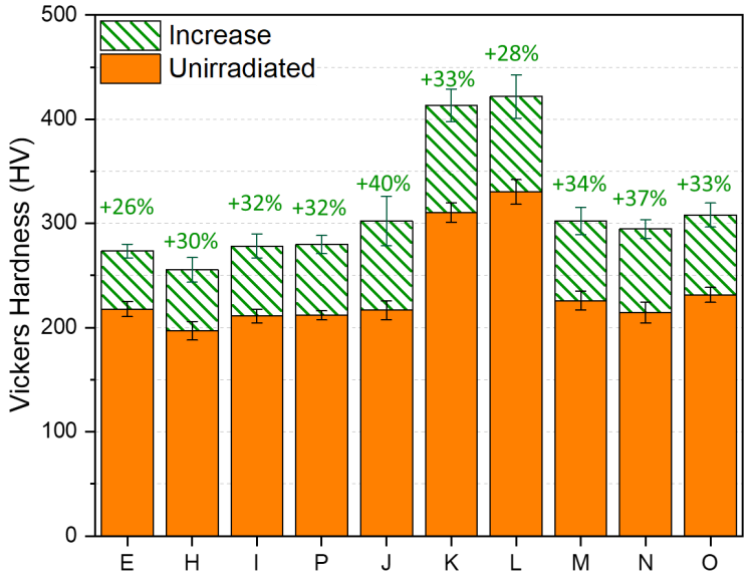

Figure 5: Increase in hardness of the ten steels after neutron irradiation at 300°C +/-30°C, 2.5 dpa. Measured on SS-J3 samples using 1 kg load, 15 s dwell time. Error bars correspond to +/- the standard deviation

3.3. Tensile properties

3.3.1. Tensile tests

Tensile tests were performed on SS-J3 tensile specimens before and after irradiation. The measured Yield Strength (YS), Ultimate tensile Strength (UTS), Uniform Elongation (UE) and Total Elongation (TE) are presented in Figure 6 for tests at 300°C. Data of the EUROFER97/2 reference material with a standard heat treatment are added for comparison.

It is evident that all the steels hardened after irradiation, reflected by an increase in the YS and UTS. This was accompanied by a decrease in UE and TE. As expected previously from the Vickers hardness results, K- and L-series steels are the strongest materials, with UTS above 800 MPa before irradiation and above 900 MPa after irradiation. The rest of the material present YS in the range 330-460 MPa in the unirradiated state, and 510-640 MPa in the irradiated state, which proves them all softer than EUROFER97/2, especially after irradiation. After irradiation, the UE of EUROFER97/2 drops to 0.2%, when for all materials of the study it remains in the range 2.5-4.5%. As the TE does not show the same tendency, these results have to be handled with care. There could be a dependency of the UE results on the size and geometry of the specimens that were used for this study.

Materials J and E behave approximately the same, with a YS of ~420 MPa and a UTS of ~520 MPa in the unirradiated state. After irradiation, J shows higher TE (+ ~3%), and higher YS and UTS (+ ~50 MPa), which is in correspondence with the previously shown hardness results.

The H-, I- and P-series steels are in the unirradiated state softer than the studied references E and J, especially H with a YS of ~330 MPa. This is attributed to their over-tempered microstructure seen in Figure 2, as well as to the lower level of carbon in material H.

Also, in terms of elongation, E performs clearly at the lower end compared to H, I, P and J. However, after irradiation, there is no dramatic deviation in UE or TE between the materials, as they all show UE between 2.5-4.5% and TE between 13-15%. The irradiated state presents no benefit of the initial high uniform elongation. Therefore, focusing on a good tensile ductility in the unirradiated state does not necessarily lead to a good tensile ductility after irradiation.

It could also be noted that the comparison of H, I and P tends to show that material P presents less irradiation induced strengthening, which could be attributed to the observed lower number density and higher size of dislocation loops compared to H and I, leading to a lower interference with the dislocation motion.

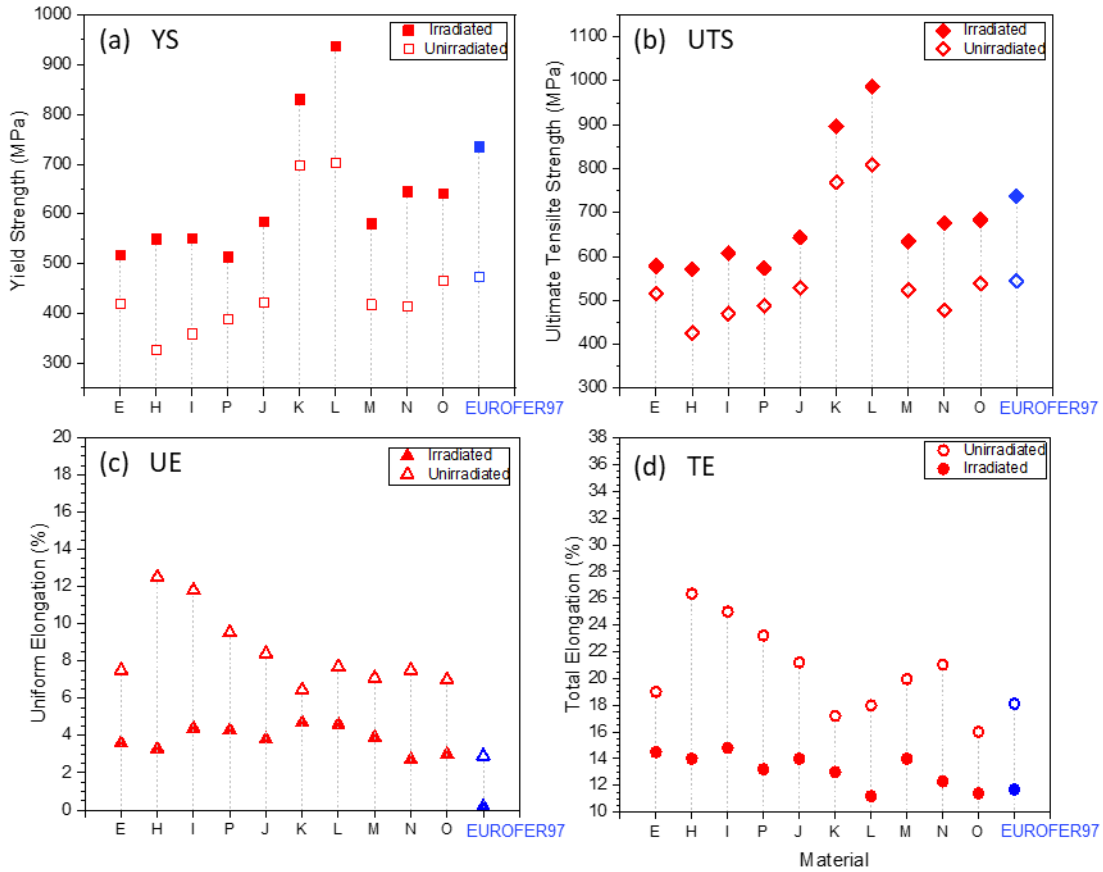

Figure 6: Tensile properties of the 10 steels measured before and after irradiation at 300°C +/-30°C, 2.5 dpa: a) Yield Strength, b) Ultimate Tensile Strength, c) Uniform Elongation and d) Total Elongation. The tests were performed at 300°C. Data from EUROFER97/2 reference material are from [18], [19].

3.3.2. Fractography

Fractography was performed on all materials after tensile testing at room temperature in both irradiated and unirradiated conditions (Table 4). Before irradiation, most materials broke in a ductile fashion, presenting a highly dimpled fracture surface, typical of ductile metals and containing cup and cone features expected due to the presence of carbides (Figure 7). For some materials (H, I, P, J and to some extent N and O), the fracture surface showed many large dimples, suggesting the presence

of a low density of large (>1 µm) inclusions in the steels (Figure 7.c). This is particularly the case in material I. These particles would be large tantalum oxide inclusions, acting as fracture initiation sites [13]. Their presence is the result of a non-optimized fabrication procedure. This problem is known in the fabrication of steels, as it appeared before in F82H and in the development of EUROFER97.

After irradiation, most materials show a consistent mode of fracture with their unirradiated form (Figure 8). However, among the softer steels, I series steel stands out because it fails mainly in a ductile fashion, but consists of some very flat regions on the fracture surface indicating evidence of cleavage fracture (Figure 8.b). This is the result of the presence of a small fraction of ferrite in the material, as seen in Figure 2.

Contrary to the other materials, material L, exhibits a mixed mode of fracture. It appears that the cracks may be running preferentially along the very large PAGs. The regions away from the brittle cleavages showed dimpled fracture typical of ductile materials but showing cup and cone fracture expected due to the presence of the carbide/nitrides. In this steel, no excessively large dimples, suggestive of inclusions, were detected on the fracture surface. After irradiation, both L and K materials exhibit this mixed mode of fracture (Figure 8.c), with a higher fraction of cleavage fracture for material K.

	Unirradiated		Irradiated
	Fracture mode	Remark	Fracture mode
E	ductile		ductile
H	ductile	Inclusions	ductile
I	ductile	Inclusions	ductile, but some flat regions indicating cleavage fracture
P	ductile	Inclusions	ductile
J	ductile	Inclusions	ductile
K	ductile		mixed mode of fracture
L	Mixed mode of fracture		mixed mode of fracture
M	ductile		ductile
N	ductile	Inclusions	ductile
O	ductile	Inclusions	ductile

Table 4: Summary of fracture modes observed via fractography on tensile specimens

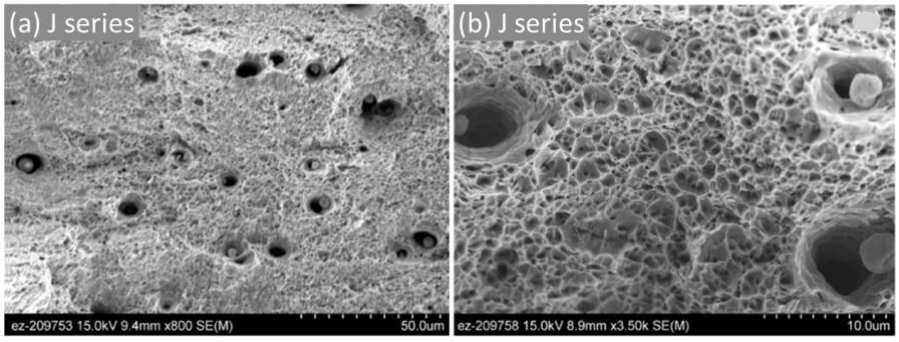

Figure 7: Fractography of J series steel after tensile tests at room temperature before irradiation (secondary electron images). (a) Inclusions on the fracture surface and (b) Ductile fracture surface with cup and cone features.

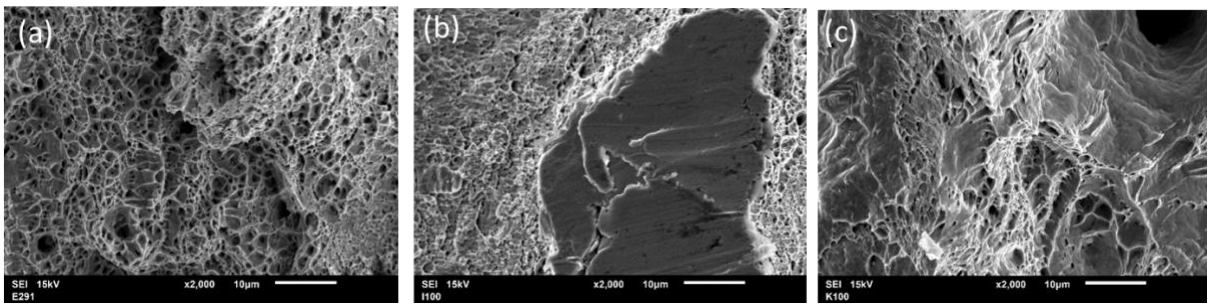

Figure 8: Fractography of irradiated tensile specimens after test at room temperature: (a) E series, (b) I series and (c) K series

3.4. Fracture toughness

Fracture toughness measurements were performed on sub-miniaturized specimens with application of the master curve approach. The values of the transition temperature T_{0Q} before and after irradiation are reported in Figure 9. Considering that the irradiation of bend bars on materials M and N failed, these results are not shown here. Data of the EUROFER97/2 reference material are added for comparison. Also, values of the DBTT from Charpy impact tests on KLST specimens of unirradiated materials are reported on the figure.

The results in Figure 9 show clearly the irradiation-induced upward shift in T_{0Q}. For the reference material EUROFER97/2, the upward shift is expected to be of about +110°C after irradiation at 300°C to 2.5 dpa [2].

Materials E (sub-optimum reference), K, and L showed a similar degree of irradiation embrittlement as the standard EUROFER97/2.

The other materials of the study (H, I, P, J, and O), however, despite their various chemical compositions and processing conditions, show less embrittlement (shift of ~50°C in T_{0Q}) and behave much better than expected. In particular, T_{0Q} for the irradiated J-material is found to be -58°C (for test temperature -125°C), which is rather promising, given that T_{0Q} for EUROFER97/2 is around 20°C [1]. It is worth noting that due to the smaller size of M4CVN specimens, most tests were performed at temperatures more than 50°C lower than T_{0Q} (T_{0Q}-50°C is the low test temperature limit per ASTM E1921) to yield reasonable number of un-censored data. Our early studies on unirradiated F82H and Eurofer 97 showed that such practice resulted in similar T_{0Q} compared with testing at the normal temperature range for larger size specimens [12], [20]–[22]. Further microstructure study is needed to understand the difference in the observed fracture toughness results.

It can also be noted that among the KIT batches, H, which was a little softer than I and P because of its lower C content, benefits of a lower T_{0Q}.

The Charpy results on KLST specimens are consistent with fracture toughness tests on miniaturized bend bars, as DBTT and T_{0Q} before irradiation follow the same tendencies for the entire test set. The DBTT for every material is about 10-60°C lower than the T_{0Q}, except for materials K and L, for which it is higher of 15-25°C, and material O for which the DBTT is close to the T_{0Q}. For EUROFER97 itself, KLST and DBTT are identical.

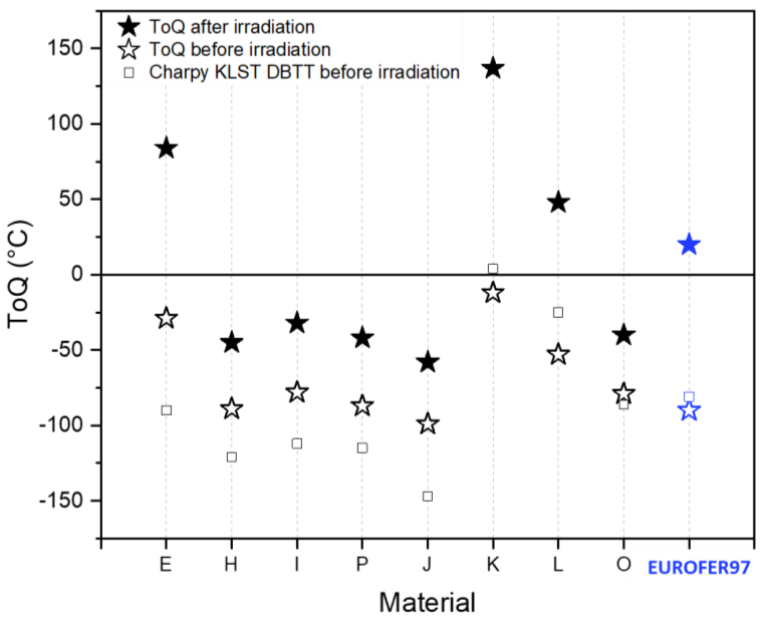

Figure 9: T_{0Q} measurements by fracture toughness tests with Master curve approach before and after irradiation at 300°C +/-30°C, 2.5 dpa. Materials M and N were excluded because of the failing irradiation temperature. Data of the EUROFER97 reference material from [1], [19] are included. For comparison purposes, the DBTT of the materials measured by Charpy test on unirradiated KLST samples, are also presented.

4. Discussion

Technological treatment

Material E is a EUROFER reference in terms of composition but was prepared in a non-conventional way. The solution annealing (or normalization), enabling all carbides to dissolve, was not performed on this material. Instead, a 'technological heat treatment' at a lower temperature was performed (980°C followed by slow air-cooling), leading carbides to grow through high temperature diffusion, in a ferritic microstructure (without martensite formation). Then the standard heat treatments of austenitization at 980°C, quenching and tempering at 760°C were performed, leading to a state of relaxed martensite, with large $M_{23}C_6$ at grain boundaries, as seen in the microstructure section (Figure 3). A homogeneous distribution of fine precipitates on these boundaries or inside grains was not obvious. These microstructure features likely resulted in the lower strength and toughness for this material.

This 'technological heat-treatment' simulates the worst-case technological situations, which could occur after welding or during problematic production steps. This off-normal case is not a standard EUROFER, but rather covers the lower range of EUROFER material properties. The results give a good approximation for what has to be expected with joints (i.e. heat treated beam welds) after irradiation compared to the base material.

SSTT sensibility

The mechanical tests performed at ORNL on SSJ3 tensile samples and bend bars on material E showed decreased properties compared to EUROFER97/2, attributed to the rather large and heterogeneous microstructure as well as the presence of the very large carbides along PAG boundaries, result of the 'technological heat treatment'. However, Charpy and tensile tests were repeated on bigger samples, showing results comparable to standard EUROFER97/2. Therefore, this shows a higher sensibility of Small Specimen Technology Tests (SSTT) to inhomogeneity in the material.

Optimum state of EUROFER

Material J (lab-cast EUROFER) is also very close to EUROFER97/2 in terms of composition, but its processing (hot-rolling) was optimized via a specific TMT process, followed by low temperature normalizing (880°C) and rather high temperature tempering (750°C). This led to improved properties compared to EUROFER97/2, with lower DBTT and much better ductility. The overall irradiation-induced deterioration of the mechanical properties is comparable to the other tested grades, but the T_{0Q} determined from the fracture toughness samples is the lowest of the test set, significantly below room temperature (-58°C).

Tolerance against ferrite fraction

The KIT batches H, I and P contained a low amount of Mn, which involves a higher transition temperature, and therefore a higher possible tempering treatment. This is why the tempering was performed at 820°C. This revealed to be at the verge of the transformation, because a small fraction of ferrite was found in materials H and I, leading to some cleavage fracture surfaces in the tensile tests after irradiation. However, even though it is well known that ferrite does not behave well under irradiation, the mechanical properties of material H, I and P were not dramatically different from the optimized reference J. Therefore, this shows that the material can accept some percentage of ferrite without dramatic consequences.

Material K

Material K was produced via the same optimized TMT process as material J, but followed by different normalizing and tempering process, and from an altered composition, with reduced Mn and Cr content, and severely reduced C content.

The material displayed a coarse microstructure, which likely resulted from the rather high normalization temperature (1050°C), and can partly explain the poor toughness results. Also, the short (15 min) and low temperature (675°C) tempering might not have produced a fully tempered martensite structure. And the very low C content could have contributed to facilitating the decomposition of martensite into ferrite and cementite phases during tempering. This would explain the higher hardness and strength of material K, but poorer fracture toughness. Also, a possible explanation to the high hardness and strength could be that due to the low C content, W might not precipitate and would stay in solid solution, leading to higher hardness. However, the contribution of precipitation strengthening compared to EUROFER97 would be significantly lower. The low carbon content also resulted in very few precipitates in this material.

The microstructural investigations on irradiated material K revealed an intense formation of dislocation loops with high density and relatively large size. Further investigations are necessary to understand what provoked this, especially as this was not the case for other TEM-probed grades (H, I, P).

Material L

Material L was initially developed for elevated temperature applications. This material received a special heat treatment with higher austenitizing temperature (1150°C) and lower tempering temperature (700°C). As in material K, this resulted in a coarse microstructure and led to higher hardness and strength but poorer toughness than the rest of the materials, even before irradiation. This material was also shown to display high creep and fatigue resistance: the ultimate tensile strength was increased by more than 200 MPa at 650°C, while the creep lifetime was improved by about 2 orders of magnitude compared to EUROFER97/2 [23]. The higher nitrogen content in this material might have further contributed to the increased hardness and strength.

Materials M, N, O

Unfortunately, the bend bar specimens of two of the three alloys provided by ENEA (M and N) underwent a higher irradiation temperature. Therefore, it was not possible to draw any conclusion concerning the irradiation embrittlement and DBTT shift at the target temperature for these alloys. However, in terms of strength and hardness, these materials exhibited similar mechanical properties compared to the references EUROFER97 of the study (E, J).

The last alloy, material O, has a reduced amount of C and Ta, and increased V and N, and was produced via a specific ausforming process with 40% reduction ratio rolling at 650°C. It was initially developed for high temperature applications, but its poor creep resistance discarded it for this use. However, considering its DBTT of –86°C in the unirradiated state, it was still considered for low temperature applications. The post-irradiation investigations proved indeed that it showed low irradiation induced embrittlement.

Impact of annealing and tempering conditions on irradiation behavior

In this work, the objective was to investigate the possibility of reducing the effect of neutron irradiation hardening and embrittlement. The strategy was to explore methods to lower the initial DBTT of EUROFER materials by thermo-mechanical optimization and chemical composition refinement. Indeed, taking previous investigations into account, the working hypothesis was that the irradiation induced shift in DBTT was about proportional to the property in the unirradiated state. That is, if a material shows a high DBTT in the unirradiated state, it will show higher DBTT shift after irradiation compared to a material with low initial DBTT. This checks out with the results of the present study: materials showing rather poor initial toughness with high T_0 (E, K, L) also show the highest level of irradiation induced T_0 shift (Figure 9).

One strategy to lower the DBTT is to lower the normalizing temperature. Indeed, Lu *et al*. showed, by comparing the microstructural properties of EUROFER97 materials prepared with normalizing temperature from 980°C to 1150°C, that a decrease in normalizing temperature involved a decrease in PAG size and an increase in low angle grain boundaries [24]. Fast cooling would also lead to higher fraction of low angle boundaries. In general, fine grain size and high fraction of low angle grain boundary are beneficial to DBTT. Fine grain sizes provide greater barriers to cleavage cracks because of the large number of crack arrests that are made. Low angle boundaries have better atomic fitting on the grain boundaries planes and this results in a greater resistance to inter-granular crack propagation. The authors of the study therefore conclude that EUROFER97 would benefit on these grounds from the lower temperature solution treatment, followed by fast cooling (air cool or water quenching). In the present study, it appears clear that the material prepared with a very low normalizing temperature (J, 880°C, Table 2) presents also the finest microstructure (Figure 2) and the best impact properties (Figure 9) both before and after irradiation. On the other hand, the materials prepared with high normalizing temperatures (K and L, 1050°C and 1150°C, respectively) present very large microstructures and behave the worst in toughness.

Another strategy to reduce the irradiation induced DBTT shift of steels can also be to control the tempering conditions. Previous studies showed that F82H steels irradiated at 250°C showed decreased DBTT shifts due to irradiation with increasing tempering temperature from 750°C to 780°C, as well as with increasing tempering time from 0.5 h to 10 h ([25], [26]). Indeed, after quenching, i.e., in the state of hard martensite, an increase in the tempering temperature or time involves higher diffusion of captured carbon to the grain boundaries, where it forms $M_{23}C_6$ precipitates. This leads to softening of the material, to lower DBTT (measured by Charpy tests or T_0 approach with fracture mechanics tests), and to higher ductility (uniform and total elongation). However, in the usual time scales for tempering (1-2 hours), the influence of time is very limited, as long as the period of tempering is sufficient to fully temper the whole sample or component. Since the diffusion is rather fast, no significant change in the microstructure after about 30 minutes would be expected. In the present study, it can be noticed that materials K and L have been processed with low tempering temperatures (675°C and 700°C, respectively, Table 2). This can further explain their poor ductility and higher strength compared to the rest of the materials. Also, materials H, I and P were tempered at high temperature (820°C), but a strong influence could not be identified compared to the rest of the materials.

Micro-alloying

In the end, despite different chemical compositions, five materials (H, I, P, J, O) present good behavior in toughness and display comparable T_0 and shift in T_{0Q}. Therefore, chemical compositions seem not to have a drastic impact on mechanical properties within these small variations. That is, these materials are comparable, and their microstructure is rather similar. However, the lower, and better, T_{0Q} and T_{0Q} shift values for J could be explained by the lower normalizing temperature and higher tempering temperature. Also, concerning material O, presenting a very comparable chemical composition with H, the slightly negative trend results could probably originate in the final rolling at a low temperature (650 °C), which would have induced a slightly different microstructure.

5. Conclusions

In this work, 10 newly developed advanced RAFM steels were irradiated at 300°C with 2.5 dpa in order to evaluate their embrittlement behavior. These materials are the result of development programs aiming at tailoring mechanical properties of EUROFER97 for high or low temperature applications in future fusion reactors. This paper presents and discusses results of the LOT-IV neutron

irradiation campaign, which are relevant to the answering of the above-mentioned questions. The results of the post irradiation examinations lead to the following conclusions:

- Compared to available EUROFER97 data, specific thermo-mechanical treatment followed by heat treatment leads to significantly better DBTT (measured by T_0) behavior after irradiation for 5 alloys.
- Micro-alloying EUROFER-type steels influences the mechanical properties. However, the effect is masked by the much stronger effect of heat treatment and fabrication history. The applied strategies of removing manganese, reducing carbon, increasing vanadium and/or nitrogen do not differ clearly enough to identify a dominating impact on irradiation damage.
- The only obvious choice for down-selection is material K (no manganese, very low carbon and reduced chromium content in combination with high temperature normalizing and very low final tempering temperature) that performed rather low in all aspects.
- Despite requiring data also at high dpa values, the results indicate that with these modified materials, an increased lifetime and potentially also an increased operating temperature window can be achieved compared to EUROFER97.
- The effect of the non-optimized technological relevant heat treatment on material E is clearly recognizable in comparison to the other alloys. But compared to the EUROFER97 data, the measured DBTT shift and the irradiation hardening are both in the same range.
- Small Specimen Test Technology is more sensitive to microstructural inhomogeneities.

Additionally, further observations were made:

- Microstructural examinations have proven that the initial microstructural conditions (PAG, block, lath structures) remained unchanged after the irradiation, as well as no evidence of any chemical re-distribution or secondary phase precipitation of any sort.
- Comparably high elongation was obtained for H, I, and P materials before irradiation, but the benefit of it was not visible after irradiation compared to the other alloys.
- A small amount of ferrite in the material did not lead to a visible negative effect on hardening or embrittlement, showing that EUROFER is tolerant against small amounts of ferrite.
- Fractography investigations revealed that large inclusions of Ta oxides appeared in some of the materials. For future productions, the Ta should be carefully introduced during fabrication.
- Even though the materials were made in a lab-facility (OCAS N.V.) and despite the detected Ta-oxides, the modified material, compared to EUROFER97, was produced in such a way that it exhibits high potential for fine tuning via subsequent processing routes.

Acknowledgements

This work has been carried out within the framework of the EUROfusion Consortium and has received funding from the Euratom research and training program 2014-2018 and 2019-2020 under grant agreement No 633053. The views and opinions expressed herein do not necessarily reflect those of the European Commission. SCK CEN acknowledges the financial support of FOD grant provided for fusion R&D. The authors also wish to thank T. Bergfeld (KIT) for the chemical analysis and D. Bolich (KIT) for the material preparation and heat treatments.

References

[1] E. Gaganidze, H.-C. Schneider, B. Dafferner, and J. Aktaa, “Embrittlement behavior of neutron irradiated RAFM steels,” *J. Nucl. Mater.*, vol. 367–370, pp. 81–85, 2007, doi: 10.1016/j.jnucmat.2007.03.163.

[2] E. Gaganidze and J. Aktaa, “Assessment of neutron irradiation effects on RAFM steels,” *Fusion Eng. Des.*, vol. 88, no. 3, pp. 118–128, 2013, doi: 10.1016/j.fusengdes.2012.11.020.

[3] J. Hoffmann, M. Rieth, M. Klimenkov, and S. Baumgärtner, “Improvement of EUROFER’s mechanical properties by optimized chemical compositions and thermo-mechanical treatments,” *Nucl. Mater. Energy*, vol. 16, pp. 88–94, 2018, doi: 10.1016/j.nme.2018.05.028.

[4] A. Di Schino, C. Testani, and L. Pilloni, “Effect of thermo-mechanical parameters on the mechanical properties of Eurofer97 steel for nuclear applications,” *Open Eng.*, vol. 8, no. 1, pp. 349–353, 2018, doi: 10.1515/eng-2018-0040.

[5] A. Puype, L. Malerba, N. De Wispelaere, R. Petrov, and J. Sietsma, “Effect of processing on microstructural features and mechanical properties of a reduced activation ferritic/martensitic EUROFER steel grade,” *J. Nucl. Mater.*, vol. 494, pp. 1–9, 2017, doi: 10.1016/j.jnucmat.2017.07.001.

[6] G. Federici, L. Boccaccini, F. Cismondi, M. Gasparotto, Y. Poitevin, and I. Ricapito, “An overview of the EU breeding blanket design strategy as an integral part of the DEMO design effort,” *Fusion Eng. Des.*, vol. 141, pp. 30–42, 2019, doi: 10.1016/j.fusengdes.2019.01.141.

[7] L. Pilloni, C. Cristalli, O. Tassa, I. Salvatori, and S. Storai, “Grain size reduction strategies on Eurofer,” *Nucl. Mater. Energy*, vol. 17, pp. 129–136, 2018, doi: 10.1016/j.nme.2018.06.023.

[8] L. Pilloni, C. Cristalli, O. Tassa, L. Bozzetto, E. Zanin, and N. Bettocchi, “Development of innovative materials and thermal treatments for DEMO water cooled blanket,” *Nucl. Mater. Energy*, vol. 19, pp. 79–86, 2019, doi: 10.1016/j.nme.2019.01.026.

[9] C. Cristalli, L. Pilloni, O. Tassa, L. Bozzetto, R. Sorci, and L. Masotti, “Development of innovative steels and thermo-mechanical treatments for DEMO high operating temperature blanket options,” *Nucl. Mater. Energy*, vol. 16, pp. 175–180, 2018, doi: 10.1016/j.nme.2018.06.016.

[10] A. A. Campbell, W. D. Porter, Y. Katoh, and L. L. Snead, “Method for analyzing passive silicon carbide thermometry with a continuous dilatometer to determine irradiation temperature,” *Nucl. Instrum. Methods Phys. Res. Sect. B Beam Interact. Mater. At.*, vol. 370, pp. 49–58, 2016, doi: 10.1016/j.nimb.2016.01.005.

[11] X. Chen *et al.*, “Mechanical properties and microstructure characterization of Eurofer97 steel variants in EUROfusion program,” *Fusion Eng. Des.*, vol. 146, pp. 2227–2232, 2019, doi: 10.1016/j.fusengdes.2019.03.158.

[12] X. Chen *et al.*, “Master Curve Fracture Toughness Characterization of Eurofer97 Steel Variants Using Miniature Multi-Notch Bend Bar Specimens for Fusion Applications,” presented at the ASME 2019 Pressure Vessels & Piping Conference, San Antonio, Texas, USA, 2019, doi: 10.1115/PVP2019-93797.

[13] A. Bhattacharya *et al.*, “Mechanical properties and microstructure characterization of unirradiated Eurofer-97 steel variants for the EUROfusion project,” ORNL/SPR--2018/882, 1471901, 2018. doi: 10.2172/1471901.

[14] R. Klueh and D. Harries, Eds., *High-Chromium Ferritic and Martensitic Steels for Nuclear Applications*. West Conshohocken, PA: ASTM International, 2001.

[15] A. Bhattacharya, C. M. Parish, J. Henry, and Y. Katoh, “High throughput crystal structure and composition mapping of crystalline nanoprecipitates in alloys by transmission Kikuchi diffraction and analytical electron microscopy,” *Ultramicroscopy*, vol. 202, pp. 33–43, 2019, doi: 10.1016/j.ultramic.2019.03.015.

[16] A. Bhattacharya, X. Chen, T. Graening, J. Reed, J. W. Geringer, and Y. Katoh, “Post-irradiation examination of Eurofer97 steel variants irradiated to 2.5 dpa, 300°C in HFIR for the EUROfusion program,” EUROfusion report Final report for task MAT-6.4.1 T001-D006, 2020.

[17] M. Rieth *et al.*, “EUROFER 97 Tensile, charpy, creep and structural tests,” Germany, 0947–8620, 2003. [Online]. Available: http://inis.iaea.org/search/search.aspx?orig_q=RN:35032617.

[18] “Material Property Handbook EUROFER97 - Grant Deliverable MAT D25.15,” EUROFusion, 2017.

[19] E. Gaganidze, “Assessment of Fracture Mechanical Experiments on Irradiated EUROFER97 and F82H Specimens,” Forschungszentrum Karlsruhe GmbH Germany, Final Report for Task TW5-TTMS 001-D14, 2007.

[20] X. Chen, M. A. Sokolov, Y. Katoh, M. Rieth, and L. N. Clowers, “Master Curve Fracture Toughness Characterization of Eurofer97 Using Miniature Multi-Notch Bend Bar Specimens for Fusion Applications,” Volume 1A: Codes and Standards, 2018, doi: 10.1115/PVP2018-85065.

[21] M. Sokolov and H. Tanigawa, “Fusion Reactor Materials Program Semiannual Progress Report,” p83, DOE/ER-0313/41, 2006.

[22] M. Sokolov and H. Tanigawa, “Fusion Reactor Materials Program Semiannual Progress Report,” p105, DOE/ER-0313/41, 2002.

[23] G. Pintsuk *et al.*, “European materials development: Results and perspective,” *Fusion Eng. Des.*, 2019, doi: 10.1016/j.fusengdes.2019.02.063.

[24] Z. Lu, R. G. Faulkner, N. Riddle, F. D. Martino, and K. Yang, “Effect of heat treatment on microstructure and hardness of Eurofer 97, Eurofer ODS and T92 steels,” *J. Nucl. Mater.*, vol. 386–388, pp. 445–448, Apr. 2009, doi: 10.1016/j.jnucmat.2008.12.152.

[25] E. Wakai *et al.*, “Effect of Initial Heat Treatment on DBTT of F82H Steel Irradiated by Neutrons,” *Fusion Sci. Technol.*, vol. 47, no. 4, pp. 856–860, May 2005, doi: 10.13182/FST05-A793.

[26] E. Wakai, N. Okubo, M. Ando, T. Yamamoto, and F. Takada, “Reduction method of DBTT shift due to irradiation for reduced-activation ferritic/martensitic steels,” *J. Nucl. Mater.*, vol. 398, no. 1–3, pp. 64–67, Mar. 2010, doi: 10.1016/j.jnucmat.2009.10.011.